Phys. Status Solidi B **250,** No. 4, 864–869 (2013) / **DOI** 10.1002/pssb.201200851

physica status solidi b
www.pss-b.com
basic solid state physics

Phase competition in $(La_{1-c},Sr_c)CoO_3$ solid solutions: *ab initio* thermodynamic study

David Fuks*[,1], Amir Weizman[1], and Eugene Kotomin[2,3]

[1] Department of Materials Engineering, Ben Gurion University of the Negev, Beer Sheva 84105, Israel
[2] Max Planck Institute for Solid State Research, Heisenbergstr. 1, 70506 Stuttgart, Germany
[3] Institute of Solid State Physics, University of Latvia, Kengaraga 8, 1063 Riga, Latvia

Received 12 October 2012, revised 13 November 2012, accepted 13 November 2012
Published online 5 April 2013

Keywords defects, DFT, perovskites, solid solutions, thermodynamics

* Corresponding author: e-mail fuks@bgu.ac.il, Phone: +972 8 6461 460, Fax +972 8 6472 946

Statistical thermodynamics and density functional theory (DFT) formalisms are combined to analyze the phase competition of energetically preferable phases in $(La_{1-c},Sr_c)CoO_3$ solid solutions upon $LaCoO_3$ doping with Sr. La/Sr sublattice in ABO_3 perovskite structure is considered as immersed in the field of CoO_3 units and the superstructures that are stable with respect to the formation of antiphase domains are analyzed. The concentration-dependent energy parameters determining the relative stability of the cubic superstructures (phases) are extracted. This allows us calculations of concentration- and temperature dependences of the long-range order (LRO) parameters for different phases. The temperatures of the order–disorder phase transformations for energetically stable at $T = 0$ K phases are obtained. It is shown that the phase corresponding to the $(La_{0.875},Sr_{0.125})CoO_3$ composition may exist at low temperatures. Nevertheless, already at room temperature it fails in the phase competition with the disordered $(La_{1-c},Sr_c)CoO_3$ solid solution and the phase corresponding to the $(La_{0.75},Sr_{0.25})CoO_3$ composition and thus hardly can be observed.

1 Introduction Mixed conducting ABO_3-type perovskites are commonly used as materials for solid oxide fuel cell (SOFC) cathodes and permeation membranes [1]. Within this class of materials, promising are cobalt-containing perovskites, *e.g.* $(La_{1-c},Sr_c)CoO_{3-\delta}$ (LSC) [2]. Variation of dopant concentration and spatial distribution over A and/or B sites of the ABO_3 perovskite structure can considerably affect functional properties of materials. The thermodynamic stability of atomic structure of such solid solutions at relatively high SOFC operation temperatures (~1100–1300 K) is of a great importance. In particular, disordering affects considerably oxygen permeability in these materials [3].

In this paper, we combine the standard density functional theory (DFT) theory with the thermodynamics of solid solutions, in order to study, how Sr alloying influences the LSC structural stability and order-disorder transformation temperature.

2 Method According to Ref. [4], both $LaCoO_3$ and $SrCoO_3$ reveal an ABO_3-type perovskite structure. $SrCoO_3$ could be grown as cubic crystals [5] whereas $LaCoO_3$ shows a small rhombohedral distortion [6–8]. (X-ray analysis of samples $La_{0.6}Sr_{0.4}CoO_{3-\delta}$ [3] indicates simple cubic symmetry.) Our calculations show that the difference between the total energies of cubic and rhombohedral structures for $LaCoO_3$ is very small (~0.006 eV atom^{-1}). In this study, we neglect this tiny effect and assume a cubic structure of the LSC, where a cubic lattice constant was re-optimized for each particular composition.

The statistical thermodynamic approach combined with an *ab initio* atomistic calculations for modeling the formation of perovskite solid solutions was discussed in detail in our previous studies of perovskite solid solutions – $(Ba,Sr)TiO_3$ and $(La,Sr)MnO_3$ – as well as TiC_cN_{1-c} compounds [9–11]. Preliminary study on LSC was presented in Ref. [12]. Briefly, we consider nine structures on La/Sr sublattice immersed in the field of the rest atoms (Co and O) [9] (see Fig. 1). The total energies of these superstructures are calculated using the DFT formalism. Full Potential Augmented Plane Waves + local orbitals (APW + lo) method is applied as implemented in WIEN-2k code [13–16]. The technical details of calculations are following. Radius of muffin-tin spheres, R_{mt}, was taken equal to 2.0 a.u. for all atoms in the supercells. The product $R_{mt}K_{max}$ that determines

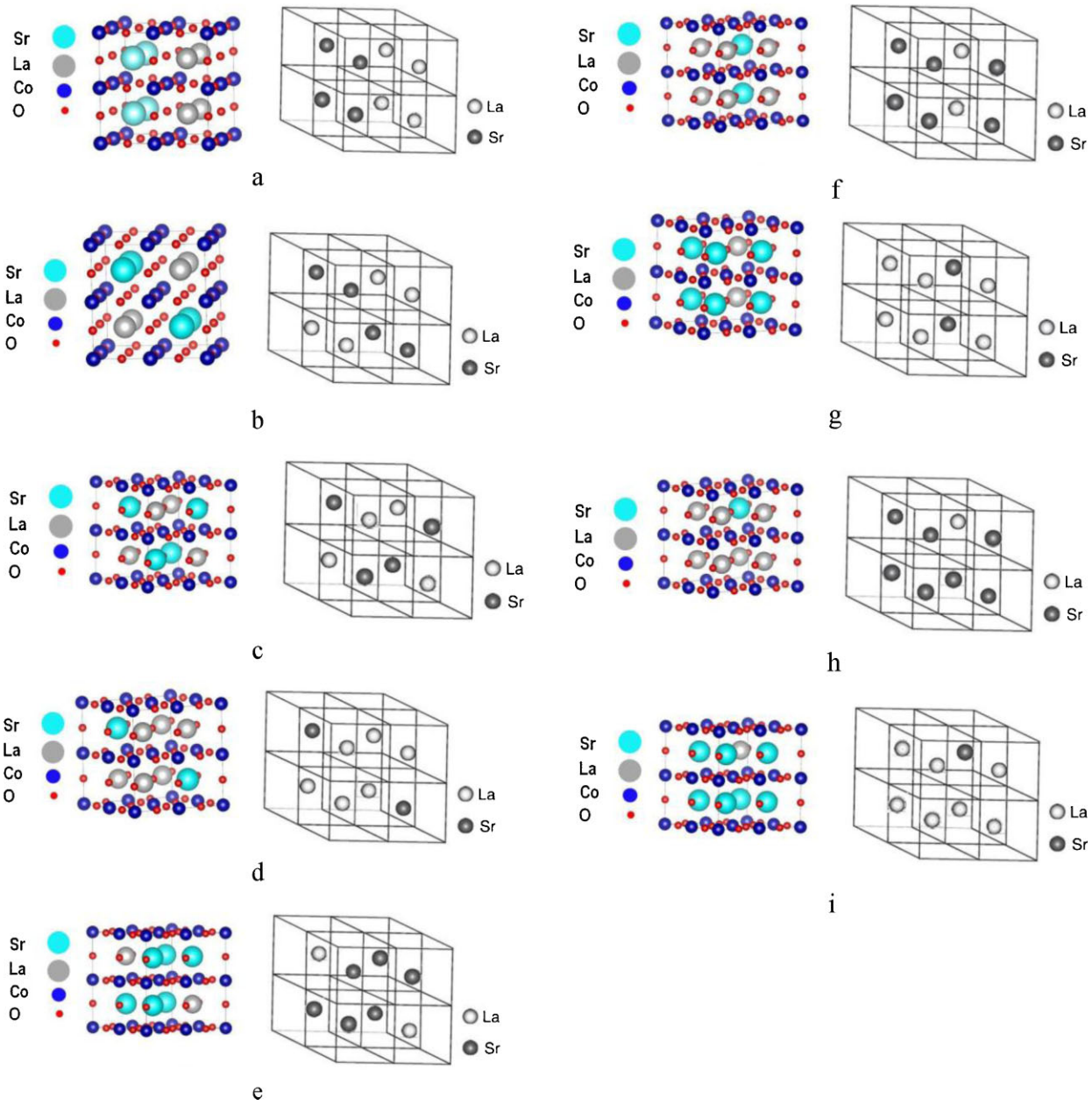

Figure 1 Superstructures (a)–(i) considered in *ab initio* calculations. The positions of La and Sr atoms on the sublattice immersed in the field of Co and O are shown in the right images.

the maximal K for basis functions was chosen equal to 6.5. The generalized gradient approximation (GGA) [17] was used for the exchange-correlation potential. The self-consistent procedure was considered as converged when the total energy in two successive steps differs by less than 10^{-3} eV. The volume optimization of all structures was carried out, to obtain the equilibrium lattice parameters and the corresponding total energies.

The structures are constructed in the framework of concentration waves theory (CW) and are stable with respect to formation of anti-site domains [18]. Free energies of these ordered structures are the functions of long-range order (LRO) parameters that describe their state of the order at different temperatures and compositions. LRO parameters are linked to the probability to find A or B atoms on the sublattice of determined type. For example, for the phase (b) from Fig. 1 in stoichiometric composition $c_{st} = 0.5$ at $T = 0$ K, the probability to find Sr atoms on their own sublattice is equal to 1 while the probability to find them on La sublattice is zero. This corresponds to the absolutely ordered state and the LRO parameter for this phase is equal to 1. When temperature increases the exchange of positions of some atoms of La and Sr on their sublattices occurs and the probability to find Sr atoms on the sites of their own

sublattice decreases leading to the decrease of the LRO parameter. The disordered state corresponds to the case when the probability to find Sr atoms on their own sublattice becomes equal to c_{st}. In this state the LRO parameter is equal to zero. Compositional disordering also may be described in terms of the same probabilities and LRO parameters. When the deviation from the stoichiometric composition in the ordering phase occurs the LRO parameter will be less than 1 even in the maximally ordered state. This state is also characterized by the probabilities to find the atoms on their own sublattices. If, let say, for considered above phase $c = 0.4$ then the probability to find Sr atoms on their own sublattice will be less than 1 while the probability to find La atoms on the Sr sublattice will be more than zero. The maximal value of LRO parameter in this case will be equal to 0.8. Increase of the temperature again will lead to the decrease of the order and LRO parameter will decrease. For mathematical details we refer to Refs. [18–20].

Keeping in mind the main aim of the research – to extract key energy parameters from the DFT calculation and to analyze the thermodynamic stability of the structures beyond $T = 0$ K, it is necessary first to determine the stable superstructures at $T = 0$ K (for this purpose the *ab initio* calculations should be carried out) and then to perform thermodynamic study for analyzing the temperature and concentration dependencies of the free energies and LRO parameters.

3 Results and discussion

3.1 Phase competition in (La,Sr)CoO_3 at $T = 0$ K Total energies of all structures from Fig. 1 and those for $LaCoO_3$ and $SrCoO_3$ were optimized with respect to the volume per atom. The number of atoms in the unit cells used in calculations for considered superstructures were equal to 10 for structures (a)–(c), 20 for structures (d)–(g), and 40 for structures (h)–(i). We calculated the superstructure formation energies which are differences of the total energies of ordered phases and two separate parent phases. A comparison of the formation energies for the superstructures is displayed in Fig. 2. It is easy to see that at the stoichiometric composition $c_{st} = 0.5$ the calculations predict the stability of the structure (b) winning the competition with structures (a) and (c). For the stoichiometric compositions $c_{st} = 0.25$ and 0.75 the formation of the structures (d) and (e) (isomorphic to phase (d) is preferable as compared with the structures (g) and (f), respectively. The straight lines show the energies of the two-phase mixtures between the corresponding phases. Also the phase (i) wins in competition with the two-phase mixture of $LaCoO_3$ and the phase (d). It is interesting to mention that although the phase (i) exists at very low temperatures, the isomorphic structure (h) does not exist even at $T = 0$ K due to the fact that it fails in the energy competition with the two-phase mixture of phases (e) and $SrCoO_3$.

3.2 Long-range order parameters To continue the analysis of the phase competition beyond $T = 0$ K, it is necessary to collect the data on the concentration and temperature dependence of the LRO parameters, η_i ($i = 1, 2, 3$) for the stable (energetically preferable) phases that are revealed above. For this purpose the free energies of formation for the phases with lowest ground state energy are used. For example, for the phases (b) and (d) these free energies have the following form [18]:

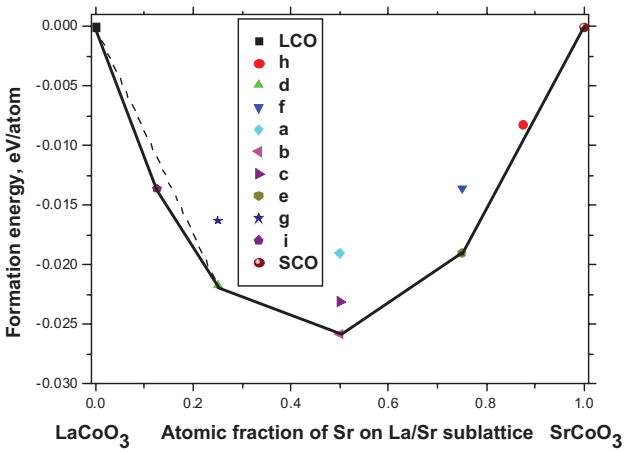

Figure 2 Formation energies for the superstructures (a)–(i) shown in Ref. [12]. Solid lines present the energies of the two-phase states between the energetically preferable phases. Dashed line presents the energy of the two-phase state – the mixture of $LaCoO_3$ and the phase (d). LCO and SCO stand for $LaCoO_3$ and $SrCoO_3$.

$$
\begin{aligned}
F_b = &-\frac{1}{2}\tilde{V}(0)c(1-c)+\frac{1}{8}\tilde{V}(2)\eta_2^2 \\
&+\frac{kT}{2}\left[\left(c+\frac{1}{2}\eta_2\right)\ln\left(c+\frac{1}{2}\eta_2\right)\right. \\
&\left.+\left(1-c-\frac{1}{2}\eta_2\right)\ln\left(1-c-\frac{1}{2}\eta_2\right)\right] \\
&+\frac{kT}{2}\left[\left(c-\frac{1}{2}\eta_2\right)\ln\left(c-\frac{1}{2}\eta_2\right)\right. \\
&\left.+\left(1-c+\frac{1}{2}\eta_2\right)\ln\left(1-c+\frac{1}{2}\eta_2\right)\right],
\end{aligned}
\tag{1}
$$

$$
\begin{aligned}
F_d = &-\frac{1}{2}\tilde{V}(0)c(1-c)+\frac{3}{32}\tilde{V}(2)\eta_2^2 \\
&+\frac{kT}{4}\left[\left(c+\frac{3}{4}\eta_2\right)\ln\left(c+\frac{3}{4}\eta_2\right)\right. \\
&\left.+\left(1-c-\frac{3}{4}\eta_2\right)\ln\left(1-c-\frac{3}{4}\eta_2\right)\right] \\
&+\frac{kT}{4}\left[3\cdot\left(c-\frac{1}{4}\eta_2\right)\ln\left(c-\frac{1}{4}\eta_2\right)\right. \\
&\left.+3\cdot\left(1-c+\frac{1}{4}\eta_2\right)\ln\left(1-c+\frac{1}{4}\eta_2\right)\right].
\end{aligned}
\tag{2}
$$

For the phase (i) the free energy of formation is much more complicated – it depends on three LRO parameters and has the form presented in Ref. [10], where the procedure of solving this equation is discussed. As may be seen from these equations they include the key energy parameters (the Fourier transforms of the mixing potentials in superstructure sites, $\boldsymbol{k}_s$ in reciprocal lattice) – $\tilde{V}(0)$, $\tilde{V}(1)$, $\tilde{V}(2)$, and $\tilde{V}(3)$, that determine the concentration and temperature dependences of the LRO parameters.

To obtain these parameters, we use the calculated DFT energies of formation for all nine superstructures and solve the set of nine equations for the energies of formation for these superstructures at stoichiometric compositions and $T = 0$ K with the unknown values of $\tilde{V}(0)$, $\tilde{V}(1)$, $\tilde{V}(2)$, and $\tilde{V}(3)$. From Fig. 2 it can be deduced that the most stable phases at $T = 0$ K are b, d, and e. Simultaneously, it is clearly seen that the formation energies for the phases d and e in stoichiometric compositions are not equal, meaning concentration dependence of the parameters $\tilde{V}(0)$ and $\tilde{V}(2)$. For this reason, as the first approximation, we assume linear concentration dependence of these interaction parameters

$$\tilde{V}(\boldsymbol{k}_s) = \tilde{V}_{11}(\boldsymbol{k}_s) + c \cdot \tilde{V}_{10}(\boldsymbol{k}_s), \tag{3}$$

with $\boldsymbol{k}_s = \frac{2\pi}{a}(000)$ or $\boldsymbol{k}_s = \frac{2\pi}{a}\left(\frac{1}{2}\frac{1}{2}0\right)$.

Keeping in mind that $\tilde{V}(0)$ is linked directly to the interaction parameter in the regular solid solution model for disordered solid solutions [21], our assumption on $\tilde{V}(0)$ corresponds to the approximation *beyond* the regular solid solution model. The concentration dependence of $\tilde{V}(2)$, in its turn, leads to the asymmetric (with respect to stoichiometric compositions) homogeneity region of the structure (b) and of the isomorphic phases (d) and (e) on the phase diagram.

Thus we have nine equations with six unknown quantities. To solve this set, the least-squares method was used to find the interaction parameters $\{V\}$ that minimize the term:

$$A * V - \Delta U, \tag{4}$$

where

$$V = \begin{pmatrix} \tilde{V}_{11}(0) \\ \tilde{V}_{10}(0) \\ \tilde{V}(1) \\ \tilde{V}_{11}(2) \\ \tilde{V}_{10}(2) \\ \tilde{V}(3) \end{pmatrix}, \quad \Delta U = \begin{pmatrix} \Delta U_1 \\ \Delta U_2 \\ \Delta U_3 \\ \Delta U_4 \\ \Delta U_5 \\ \Delta U_6 \\ \Delta U_7 \\ \Delta U_8 \\ \Delta U_9 \end{pmatrix}. \tag{5}$$

Table 1 The calculated interaction parameters.

mixing potential (eV atom^{-1})	$\tilde{V}_{10}(\boldsymbol{k}_s)$	$\tilde{V}_{11}(\boldsymbol{k}_s)$
$\tilde{V}(0)$	4.0×10^{-3}	-3.13×10^{-3}
$\tilde{V}(1)$	–	-1.29×10^{-1}
$\tilde{V}(2)$	3.02×10^{-2}	-1.98×10^{-1}
$\tilde{V}(3)$	–	-1.62×10^{-1}

Here ΔU_i are the energies of superstructure formation and A is the matrix of numerical coefficients that are determined in Ref. [9]. The results obtained by applying this procedure are given in Table 1.

It is important to mention that although the CW theory is formulated in the framework of the assumption of pairwise interactions, actually the suggested way to derive these parameters from the *ab initio* self-consistent calculations means that all non-pairwise interactions that may be reduced to pairwise interactions are included in the consideration [21]. With the set of the energy parameters $\{\tilde{V}\}$ in hand, it is possible now to analyze the temperature dependences of the free energies of ordering, $\Delta F = F_{\text{ordered}} - F_{\text{disordered}}$, for the superstructures energetically preferable at $T = 0$ K.

As an example of such an analysis, the temperature dependence for ΔF for the structures (b) and (d) in stoichiometric compositions is discussed in Ref. [12]. It was shown that the order–disorder phase transformation for the structure (b) is of the second order, while for the structures (d) and (e) the phase transformation is of the first order. For the phases (b), (d), (e) in stoichiometric compositions the phase transformation occurs at $T = 540$, 450, and 420 K, respectively.

3.3 Analysis of the stability of different phases To analyze the stability of the phases at different temperatures and concentrations, the concentration- and temperature dependence of the LRO parameters corresponding to the equilibrium should be collected by solving the following equation:

$$\left(\frac{\partial F}{\partial \eta}\right)_{\eta=\eta_{\text{eq}}} = 0. \tag{6}$$

Using this equation, the temperature dependence of the LRO parameters for each concentration on La/Sr sublattice for competing phases was obtained. Analogous procedure was used also to get $\eta_1(T)$, $\eta_2(T)$, $\eta(T)$ for the phase with the structure (i). In the latter case the procedure of the minimization of $F(\eta_1, \eta_2, \eta_3, c, T)$ with respect to *three* LRO parameters was applied. With these data in hands it is possible to calculate the concentration dependencies of the free energies of phase formation by substituting $\eta_{\text{eq}}(T)$ for η in Eqs. (1), (2) for the free energies.

Figure 3 shows the free energies of ordering for the phases (b), (d), (e), and (i) and the free energy of mixing for

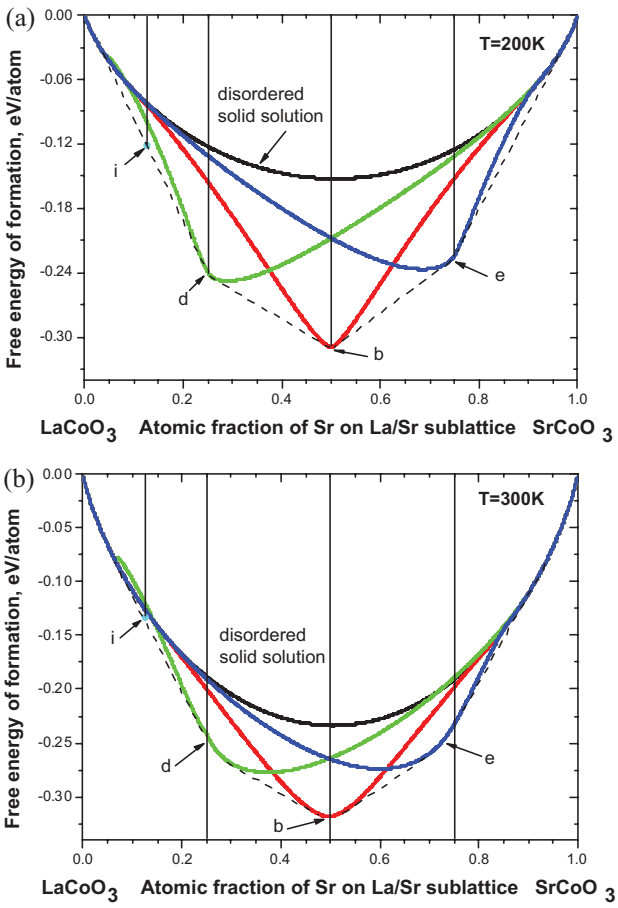

Figure 3 Free energy diagrams illustrating the phase competition at $T = 200\,K$ (a) and $T = 300\,K$ (b). For explanations see the text.

the disordered solid solution as the functions of the atomic fraction of Sr on La/Sr sublattice for two different temperatures. The vertical solid lines show the stoichiometric compositions of the corresponding phases. The tangents given by the dashed lines determine the homogeneity regions and the two-phase states (mixture of the phases).

The formation energy for the disordered solid solution is presented by the curve that is asymmetric with respect to $c = 1/2$, because $\tilde{V}(0)$ is the linear function of a composition (Eq. (3)). The phases (b), (d), and (e) also have asymmetric regions of homogeneity. For the phase (b) this happens due to the concentration dependence of the energy parameters $\tilde{V}(0)$ and $\tilde{V}(2)$. For the phases (d) and (e) the reason for such a behavior is twofold. On one hand, it is known that the maximal values of the LRO parameter in phases (d) and (e) show the asymmetric behavior when the deviation from the stoichiometric compositions in these phases ($c_{st} = 0.25$ and 0.75, respectively) occurs [19].

On the other hand, additional concentration dependence of the LRO parameter for these phases appears due to the concentration dependence of $\tilde{V}(2)$. The calculations show that the temperature of the order–disorder phase transformation for the phase (i) is relatively small and this phase fails in competition with the two-phase heterogeneous mixture of the disordered solid solution on La/Sr sublattice and the phase (d) in non-stoichiometric composition. This occurs at low (room) temperatures, as may be seen from the comparison of the position of the point presenting the formation energy of the phase (i) with respect to the tangent that determine the two-phase mixture of the disordered solid solution and the structure (d) (Fig. 3a, b).

It would be difficult to achieve the equilibrium state at such low temperature, and thus this phase can hardly be observed experimentally. There is still a room for more detailed analysis of the phase competition in the vicinity of the temperatures of the order–disorder phase transformations.

Actually, in this paper the mean field approximation was applied that does not allow us an accurate prediction of the two-phase regions at relatively high temperatures. In this case the Monte Carlo (MC) approach would be preferable, giving the correct information about the positions of the lines separating the homogeneity regions of the phases on the phase diagram. The approach suggested here allows us the investigation in this direction.

Finally, we neglected an oxygen deficiency in $LaCoO_3$, $SrCoO_3$, and in LSC phases. When atomic fraction of Sr on La/Sr sublattice grows, it may stimulate the increase of oxygen vacancy concentration. In this case, a simple quasi-binary phase diagram would be not enough to give relevant information on the phase competition. In its turn, ternary phase diagram could be useful but demanding a large amount of time-consuming *ab initio* calculations.

The attempt to discuss the decomposition in terms of simplistic quarternary phase diagram for the cubic perovskite-type oxide $Ba_xSr_{1-x}Co_{0.8}Fe_{0.2}O_{3-\delta}$ (BSCF) for specific temperature was reported recently in Ref. [22].

4 Conclusions In this paper, we studied the doping effects in technologically important $LaCoO_3$ perovskite. Detailed *ab initio* thermodynamic investigation of the phase competition in $La_{1-c}Sr_cCoO_3$ solid solutions was carried out, using the supercell approach. The possibility to link the DFT calculations for perfectly ordered phases with the analysis of non-stoichiometric phases is demonstrated. *Ab initio* analysis shows the existence of the ordered phases at $T = 0\,K$.

Special attention was paid to the analysis of the concentration dependence of the Fourier transforms of mixing potentials that determine the relative stability of different phases and the temperatures of the order–disorder transformations. For the ordered phases (b), (d), (e) in stoichiometric compositions the order–disorder phase transformation occurs at: $T = 540\,K$ ($La_{0.5}Sr_{0.5}CoO_3$), $T = 450\,K$ ($La_{0.75}Sr_{0.25}CoO_3$), and $T = 420\,K$ ($La_{0.25}Sr_{0.75}CoO_3$), respectively.

Moreover, $La_{0.875}Sr_{0.125}CoO_3$ phase may exist only at extremely low temperatures but hardly observed due to

frozen kinetics of its formation. The $La_{0.75}Sr_{0.25}CoO_3$ and the $La_{0.25}Sr_{0.75}CoO_3$ phases exist in the narrow homogeneity region and a first-order phase transformation takes place to the disordered solid solutions [12]. Lastly, the $La_{0.5}Sr_{0.5}CoO_3$ (phase b) shows the second-order phase transformation at the stoichiometric composition. Above ~550 K, the LSC system becomes disordered on the (La, Sr) perovskite sublattice for all Sr concentrations.

The obtained results could be used for more realistic modeling of oxygen transport in SOFCs.

Acknowledgements This work was supported by the GIF research project 1-1025-5-10/2009. D. F. holds the Stephen and Edith Berger Chair in Physical Metallurgy. Authors are indebted to J. Maier, R. Merkle, G. Gryaznov for stimulating discussions.

References

[1] A. Chroneos, B. Yildiz, A. Tarancón, D. Parfitt, and J. A. Kilner, Energy Environ. Sci. **4**, 2774 (2011).
[2] E. A. Kotomin, Yu. Mastrikov, R. Merkle, M. M. Kuklja, A. Roytburd, and J. Maier, Solid State Ion. **188**, 1 (2011). R. Merkle, Yu. Mastrikov, E. A. Kotomin, M. M. Kulkja, and J. Maier, J. Electron. Chem. Soc. **159**, B219 (2012).
[3] H. Kruidhof, H. J. M. Bouwmeester, R. H. E. van Doorn, and A. J. Burggraaf, Solid State Ion. **63–65**, 816 (1993).
[4] G. H. Jonker and J. H. Van Santen, Physica **19**, 120 (1953).
[5] Y. Long, Y. Kaneko, S. Ishiwata, Y. Taguchi, and Y. Tokura, J. Phys.: Condens. Matter **23**, 245601 (2011).
[6] F. Askham, I. Fankuchen, and R. Ward, J. Am. Chem. Soc. **72**, 3799 (1950).
[7] Y.-L. Lee, J. Kleis, J. Rossmeisl, Y. Shao-Hornc, and D. Morgan, Energy Environ. Sci. **4**, 3966 (2011).
[8] R. Le Toquin, W. Paulus, A. Cousson, C. Prestipino, and C. Lamberti, J. Am. Chem. Soc. **128**, 13161 (2006).
[9] D. Fuks, S. Dorfman, S. Piskunov, and E. Kotomin, Phys. Rev. B **71**, 014111 (2005).
[10] D. Fuks, L. Bakaleinikov, E. A. Kotomin, J. Felsteiner, A. Gordon, R. A. Evarestov, D. Gryaznov, and J. Maier, Solid State Ionics **177**, 217 (2006).
[11] D. Vingurt and D. Fuks, Intermetallics **18**, 359 (2010).
[12] A. Weizman, D. Fuks, E. A. Kotomin, and D. Gryaznov, Solid State Ion. **230**, 32 (2013).
[13] W. Kohn and P. Vashishta, General density functional theory, in: Theory of the Inhomogeneous Electron Gas, edited by S. Lundqvist and N. H. March (Plenum, New York, 1983), pp. 79–147.
[14] W. Kohn, A. D. Becke, and R. G. Parr, J. Phys. Chem. **100**, 12974 (1996).
[15] K. Schwarz, P. Blaha, and G. K. H. Madsen, Comput. Phys. Commun. **147**, 71 (2002).
[16] S. Cottenier, Density Functional Theory and the Family of (L)APW Methods: A Step-by-Step Introduction (Instituut Voor Kern-en Stralingsfysica, K.U. Leuven, Belgium, 2002).
[17] J. P. Perdew, K. Burke, and M. Ernzerhof, Phys. Rev. Lett. **77**, 3865 (1996).
[18] A. G. Khachaturyan, Theory of Phase Transformations in Solids (Wiley, New York, 1983).
[19] M. A. Krivoglaz and A. A. Smirnov, The Theory of Order-Disorder in Alloys (Macdonald & Co, London, 1964), p. 427.
[20] J. W. Christian, The Theory of Transformations in Metals and Alloys (Part I + II) (Pergamon, Oxford, 2002), p. 1200.
[21] Yu. F. Zhukovskii, E. Kotomin, D. Fuks, S. Dorfman, A. M. Stoneham, and G. Borstel, J. Phys.: Condens. Matter **16**, 4881 (2004).
[22] D. N. Mueller, R. A. De Souza, Th. E. Weirich, D. Roehrens, J. Mayer, and M. Martin, Phys. Chem. Chem. Phys. **12**, 10320 (2010).